An Explicit and Unconditionally Stable FDTD Method for Electromagnetic Analysis

Md. Gaffar and Dan Jiao, *Senior Member, IEEE*

***Abstract*—In this paper, an explicit and unconditionally stable finite-difference time-domain (FDTD) method is developed for electromagnetic analysis. Its time step is not restricted by the space step, and its accuracy is ensured for the time step chosen based on accuracy. The strength of the conventional explicit FDTD is thus preserved in avoiding a system matrix solution, while the shortcoming of the conventional FDTD is eliminated in the time step's dependence on space step. Numerical experiments in both 2-D and 3-D simulations have demonstrated the performance of the proposed method in stability and efficiency without sacrificing accuracy.**

***Index Terms*—Explicit methods, finite-difference time-domain (FDTD) method, unconditionally stable methods.**

I. Introduction

THE finite-difference time-domain (FDTD) method [1], [2] is one of the most popular computational electromagnetic methods for solving Maxwell's equations. It has been widely adopted by researchers in numerous science and engineering disciplines. An explicit FDTD method is free of matrix solutions. However, its time step is dependent on the space step for stability. When there exist fine features relative to the working wavelength, the time step required for stability can be much smaller than the time step determined by accuracy, which can render an explicit FDTD simulation highly inefficient.

In recent years, many unconditionally stable FDTD methods have been developed such as the alternating direction implicit (ADI)-FDTD [3]–[5], the Crank–Nicolson (CN)-FDTD [6], the locally one-dimensional (LOD)-FDTD [7], the Laguerre-FDTD [8], a series of fundamental schemes [9], and others. All of these methods are implicit methods that require a system matrix solution. It has also been observed from many existing implicit FDTD methods that the accuracy degrades greatly when using a time step much larger than that permitted by stability. In fluid dynamics, researchers have filtered unstable high-frequency waves to enlarge the time step of an explicit scheme [10]. Recently, a filtering technique has also been reported in [11] and [12], where the time step of an explicit FDTD is successfully extended beyond the CFL limit, although the method has not been made unconditionally stable. In [13], an explicit and unconditionally stable time-domain finite-element method (TDFEM) is successfully created (the preliminary work of [13] has been shown in [14] and [15]). In this method, we retain the strength of an explicit TDFEM in avoiding solving a matrix equation, and we eliminate its shortcoming in time step. Despite the success in the TDFEM, as yet no explicit FDTD methods have been made unconditionally stable.

The contribution of this paper is the successful development of an explicit and unconditionally stable FDTD method for general electromagnetic analysis involving arbitrary structures, inhomogeneous materials, and absorbing boundary conditions (ABCs) such as a perfectly matched layer (PML). The basic idea of this work has been presented in [16]. In this paper, we provide a comprehensive description of this method.

The organization of this paper is as follows. In Section II, we analyze the root cause of an explicit FDTD method when using a time step beyond the stability criterion, based on which we reveal how to make an explicit FDTD unconditionally stable. In Section III, we propose an explicit and unconditionally stable FDTD method. The matrix-free strength of the traditional explicit FDTD method is retained by the proposed method. In Section IV, we provide a detailed complexity and accuracy analysis of the proposed algorithm. In Section V, we discuss the computational efficiency of the proposed method and the terminology used to describe the proposed method. Through comparisons with the traditional explicit FDTD method in numerous 2-D and 3-D examples in both closed- and open-region settings, Section VI demonstrates the stability, accuracy, and efficiency of the proposed method. Section VII relates to our conclusions.

II. On the Root Cause of the Instability of an Explicit FDTD

In this section, we analyze the root cause of the instability of an explicit FDTD method when a time step beyond the Courant–Friedrichs–Lewy (CFL) condition is used. Existing stability analysis such as the complex-frequency analysis [2], the well-known Von Neumann analysis, and the eigenvalue-based approach for analyzing stability [18], [19] have all shed light on such a root-cause analysis. Here, we present our new findings on the root cause of instability, which enable the removal of the root cause without sacrificing accuracy in the explicit FDTD-based simulation of general electromagnetic problems.

Manuscript received February 01, 2014; revised April 22, 2014, July 18, 2014, and August 27, 2014; accepted September 01, 2014. Date of publication September 25, 2014; date of current version November 03, 2014. This work was supported by the National Science Foundation (NSF) under Grant 1065318 and by the Office of Naval Research (ONR) under Grant N00014-10-1-0482.

The authors are with the School of Electrical and Computer Engineering, Purdue University, West Lafayette, IN 47907 USA (e-mail: djiao@purdue.edu).

Color versions of one or more of the figures in this paper are available online at http://ieeexplore.ieee.org.

Digital Object Identifier 10.1109/TMTT.2014.2358557

A. Proposed Root-Cause Analysis

In an explicit FDTD method, the time marching is performed in a leapfrog manner, which yields, in a source-free region,

$$\begin{aligned} H^{n+\frac{1}{2}} &= H^{n-\frac{1}{2}} - \Delta t \mathbf{D}_E E^n \\ E^{n+1} &= E^n + \Delta t \mathbf{D}_H H^{n+\frac{1}{2}} \end{aligned} \tag{1}$$

where Δt is the time step, superscript such as $n, n \pm \frac{1}{2}$, and $n+1$ denotes the time instant, E represents the vector of the unknown electric fields in the computational domain, whereas vector H contains discretized unknown magnetic fields. $\mathbf{D}_H$ and $\mathbf{D}_E$ are sparse matrices, with matrix–vector products $\mathbf{D}_H H$ and $\mathbf{D}_E E$ representing discretized $(\nabla \times \mathbf{H})/\varepsilon$, and $(\nabla \times \mathbf{E})/\mu$, respectively. Once a space discretization is done, $\mathbf{D}_H$ and $\mathbf{D}_E$ are determined regardless of time.

Substituting the H's equation into the E's equation in (1) and rewriting (1) in a matrix form, we obtain

$$\begin{bmatrix} H^{n+\frac{1}{2}} \\ E^{n+1} \end{bmatrix} = \begin{bmatrix} \mathbf{I} & -\Delta t \mathbf{D}_E \\ \Delta t \mathbf{D}_H & \mathbf{I} - \Delta t^2 \mathbf{M} \end{bmatrix} \begin{bmatrix} H^{n-\frac{1}{2}} \\ E^n \end{bmatrix} \tag{2}$$

where

$$\mathbf{M} = \mathbf{D}_H \mathbf{D}_E. \tag{3}$$

Let

$$\mathbf{G} = \begin{bmatrix} \mathbf{I} & -\Delta t \mathbf{D}_E \\ \Delta t \mathbf{D}_H & \mathbf{I} - \Delta t^2 \mathbf{M} \end{bmatrix} \quad U^n = \begin{bmatrix} H^{n-\frac{1}{2}} \\ E^n \end{bmatrix}. \tag{4}$$

Equation (2) can be rewritten as

$$U^{n+1} = \mathbf{G} U^n. \tag{5}$$

To make the above stable, the spectral radius of $\mathbf{G}$ must be bounded by 1, i.e., the maximum modulus of the eigenvalues and thereby the modulus of all eigenvalues of $\mathbf{G}$ must be bounded by 1. To analyze the spectral radius of $\mathbf{G}$, we consider the following eigenvalue problem:

$$\mathbf{G}\mathbf{V} = \mathbf{V}\mathbf{\Lambda}_{\mathbf{G}} \tag{6}$$

where $\mathbf{\Lambda}_{\mathbf{G}}$ is the diagonal matrix comprising the eigenvalues of $\mathbf{G}$, and $\mathbf{V}$ is the matrix whose column vectors are the eigenvectors of $\mathbf{G}$.

Equation (6) can be rewritten as

$$(\mathbf{G} - \mathbf{I})\mathbf{V} = \mathbf{V}(\mathbf{\Lambda}_{\mathbf{G}} - \mathbf{I}). \tag{7}$$

Substituting $\mathbf{G}$ in (4) into the above, we obtain

$$\begin{pmatrix} 0 & -\Delta t \mathbf{D}_E \\ \Delta t \mathbf{D}_H & -\Delta t^2 \mathbf{M} \end{pmatrix} \begin{pmatrix} \mathbf{V}_H \\ \mathbf{V}_E \end{pmatrix} = \begin{pmatrix} \mathbf{V}_H \\ \mathbf{V}_E \end{pmatrix} \tilde{\Lambda}_{\mathbf{G}} \tag{8}$$

where $\mathbf{V}_H$ is the upper block of $\mathbf{V}$, the row dimension of which is the same as that of $\mathbf{D}_E$, $\mathbf{V}_E$ is the remaining part of $\mathbf{V}$, and

$$\tilde{\mathbf{\Lambda}}_{\mathbf{G}} = (\mathbf{\Lambda}_{\mathbf{G}} - \mathbf{I}). \tag{9}$$

Equation (8) can further be written as

$$-\Delta t \mathbf{D}_E \mathbf{V}_E = \mathbf{V}_H \tilde{\Lambda}_{\mathbf{G}} \tag{10}$$

$$\Delta t \mathbf{D}_H \mathbf{V}_H - \Delta t^2 \mathbf{M} \mathbf{V}_E = \mathbf{V}_E \tilde{\Lambda}_{\mathbf{G}}. \tag{11}$$

Multiplying (11) from right by $\tilde{\Lambda}_{\mathbf{G}}$ and substituting (10) into (11), we obtain

$$-\Delta t^2 \mathbf{M} \mathbf{V}_E - \Delta t^2 \mathbf{M} \mathbf{V}_E \tilde{\Lambda}_{\mathbf{G}} = \mathbf{V}_E \tilde{\Lambda}_{\mathbf{G}}^2 \tag{12}$$

which yields

$$-\Delta t^2 \mathbf{M} \mathbf{V}_E (\mathbf{I} + \tilde{\Lambda}_{\mathbf{G}}) = \mathbf{V}_E \tilde{\Lambda}_{\mathbf{G}}^2. \tag{13}$$

Denoting the ith eigenvalue of $\mathbf{G}$ by γ_i, and the ith column of $\mathbf{V}_E$ by $\mathbf{V}_{E,i}$, from (9) and (13), we have

$$-\Delta t^2 \mathbf{M} \mathbf{V}_{E,i} = \frac{(\gamma_i - 1)^2}{\gamma_i} \mathbf{V}_{E,i}. \tag{14}$$

Denoting the eigenvalues of $\mathbf{M}$ by ξ_i, it is evident from (14) that

$$-\Delta t^2 \xi_i = \frac{(\gamma_i - 1)^2}{\gamma_i}. \tag{15}$$

It can then be readily deduced from (15) that if and only if the following condition is satisfied:

$$\Delta t^2 \xi_i \le 4, \qquad i = 1, 2, \ldots, N \tag{16}$$

$|\gamma_i| \le 1$ is guaranteed, thus the spectral radius of $\mathbf{G}$ is bounded by 1, and (5) is always stable. The above condition has also been shown in [18]. In addition, as theoretically expected, (16) is the same as the condition derived in [13] although the time-domain finite-element-based marching in [13] is directly performed on a second-order vector wave equation without using the leapfrog scheme in the FDTD.

Next, we will proceed to analyze the root cause of the instability. First, we need to realize that the solution of E at any time instant can be superposed from the eigenvectors of $\mathbf{M}$, i.e., the column vectors in $\mathbf{V}_E$, as shown in (14). To explain, we can rewrite (1) as

$$\begin{aligned} \frac{\partial H}{\partial t} &= -\mathbf{D}_E E \\ \frac{\partial E}{\partial t} &= \mathbf{D}_H H \end{aligned} \tag{17}$$

Taking the time derivative of the second equation in (17) and substituting the first equation, we obtain

$$\frac{\partial^2 E}{\partial t^2} = -\mathbf{D}_H \mathbf{D}_E E = -\mathbf{M} E. \tag{18}$$

Similar to the analysis in [13], the solution of E to the above equation at any time instant resides in the eigenspace of $\mathbf{M}$. In other words, the eigenvectors of $\mathbf{M}$ form a complete and accurate set of basis functions to represent the space dependence of the field solution E at any time. A similar concept was also presented in [20]. Notice that the eigenvector of $\mathbf{M}$, i.e., the eigenmode of $\mathbf{M}$, is *not* a spatial Fourier mode. The spatial Fourier mode can be viewed as a source-free solution of

Maxwell's equations in free space, whereas the eigenmode of $\mathbf{M}$ is the resonance mode in the given problem since an eigenmode $\mathbf{V}_{E,i}$ satisfies $(\mathbf{M}-\xi_i\mathbf{I})\mathbf{V}_{E,i}=0$. Such a solution satisfies all the boundary conditions at the material interface present in the given problem. Expanding E in space by $\mathbf{V}_E$ that is composed of all the $\mathbf{M}$'s eigenvectors, we have

$$E=\mathbf{V}_E y(t) \tag{19}$$

where the space dependence of E is carried by $\mathbf{V}_E$, and the time-dependent coefficient vector $y(t)$ can be found as follows. Substituting the above (19) into (18), and front multiplying (18) by $\mathbf{V}_{E,i}^T$, we obtain

$$\frac{\partial^2 y_i}{\partial t^2}+\xi_i y_i=0.$$

As a result, we obtain the ith entry of vector $y(t)$ as the following:

$$y_i(t)=a_i\cos(\sqrt{\xi_i}t)+b_i\sin(\sqrt{\xi_i}t) \tag{20}$$

where a_i and b_i are arbitrary constant coefficients.

From (18), it can also be seen that $\mathbf{M}$ corresponds to the discretized $(1)/(\varepsilon)\nabla\times(1)/(\mu)\nabla\times$ operator. This operator is semi-positive definite. Numerically, $\mathbf{M}$ is a semi-positive definite matrix. Its eigenvalues ξ_i are hence non-negative real numbers. In addition, as can be seen from (20), $\sqrt{\xi_i}$ is nothing but the resonance frequency of the ith eigenmode in time.

Now, we have the following findings. First, (16) shows that no matter how large the time step Δt is, when instability occurs, among all the eigenmodes (eigenvectors of $\mathbf{M}$) contained in the field solution, not all of them are unstable. Only a subset of the eigenmodes that violate (16) are unstable, whereas the rest of the eigenmodes are stable. For example, the null-space modes of $\mathbf{M}$ are always stable since their eigenvalues ξ_i are zero. Second, (16) shows that the unstable modes are also those modes that cannot be accurately simulated by the given time step since $\sqrt{\xi_i}$ is nothing but the resonance frequency of an eigenmode. When (16) is violated, the frequency is too high to be accurately sampled by the given Δt, thus causing instability.

As a result of the aforementioned root-cause analysis, we conclude that the root cause of the instability of an explicit FDTD method when using a time step beyond the CFL condition is the set of the eigenmodes of $\mathbf{M}$ resulting from space discretization, whose resonance frequency is higher than what can be accurately sampled by the given time step. The number of such modes is finite since the size of $\mathbf{M}$ is finite. These unstable modes exist due to fine discretizations relative to the working wavelength. When the space discretization is finer, the eigenvalues of $\mathbf{M}$ are higher. Such a fine discretization is unavoidable in structures whose fine features are small compared to the working wavelength. It is very important to realize that the unstable modes arise from space discretization irrespective of time stepping. Once the space discretization is finer than that permitted by the given time step for accuracy, the unstable eigenmodes whose eigenvalues violate (16) exist irrespective of the methods used for time marching. That is why in an implicit method, the error amplification factor must be bounded by 1 to suppress the instability since the root cause of instability is not removed in an implicit method.

However, (16), (19), and (20) clearly suggest an alternative way to achieve unconditional stability without resorting to an implicit method. It shows that if the time step is determined by accuracy, then the unstable modes are also not required by accuracy because the frequency corresponding to these modes is beyond the highest frequency required to be captured by the given time step. To explain, assuming the maximum frequency present in a system response is $f_{\max}$. To achieve good accuracy, we at least have to choose

$$\Delta t<\frac{1}{2f_{\max}}. \tag{21}$$

The unstable modes then have frequencies

$$\sqrt{\xi_i}>\frac{2}{\Delta t}>4f_{\max} \tag{22}$$

thus beyond the maximum frequency required to be captured by accuracy.

In addition, (16) also shows that traditional CFL condition essentially requires the time step be chosen in such a way that all modes can be stably simulated by the given time step. In other words, the time step determined from the CFL condition makes (16) satisfied for all eigenmodes since the maximal $\sqrt{\xi_i}$ is inversely proportional to the smallest space step.

B. Comparison With Von Neumann Type Analysis

From the above section, it can be seen that the proposed root-cause analysis is based on the following expansion to represent the source-free solution of Maxwell's equations:

$$E(\vec{r},t)=\sum_{i=1}^{k}V_{E,i}(\vec{r})[a_i\cos(\sqrt{\xi_i}t)+b_i\sin(\sqrt{\xi_i}t)].$$

In contrast, in the complex-frequency or Von Neumann analysis, the solution at any point and any time is expanded by Fourier modes

$$E(\vec{r},t)=\sum_{i=1}^{N}\{e^{j\vec{k}_i\cdot\vec{r}}\}\,[F(k_i,t)]$$

where F is the spatial Fourier coefficient, which is time dependent, and $\{e^{j\vec{k}_i\cdot\vec{r}}\}$ denotes a spatial Fourier mode.

Comparing the two expansions, first, it is clear that each eigenmode $V_{E,i}$ is not a single Fourier mode. In fact, in a general problem with inhomogeneous materials and structures, $V_{E,i}$ has a complicated space dependence. One $V_{E,i}$ mode would have to be represented by many spatial Fourier modes. Second, given any band-limited (with respect to prescribed accuracy) input spectrum, the eigenmodes whose oscillation frequencies $\sqrt{\xi_i}$ larger than required by accuracy can be truncated without affecting accuracy. In contrast, a Fourier expansion does not show how to truncate high-frequency spatial modes without sacrificing accuracy in a general non-free-space problem.

To see the difference more clearly, take the nullspace eigenmode as an example whose $\sqrt{\xi_i}$ is zero. In the proposed root-cause analysis, this mode can be stably simulated using an arbitrarily large time step. In contrast, using the Von Neumann

analysis, this single null-space eigenmode can have many high spatial frequency components since the null-space eigenmode is the static field distribution in the given problem, and a static field distribution can also have very sharp space variations due to complicated conductor and dielectric configurations in the given problem. Using the Von Neumann or complex-frequency analysis, such a null-space eigenmode cannot be stably simulated by using an arbitrarily large time step, which is different from what is found by the proposed root-cause analysis. Certainly, in free space, the eigenmodes of $\mathbf{M}$ would revert to the Fourier modes. The two analyses then agree with each other. But, this is not true for general problems involving inhomogeneous materials and complicated structures.

III. Proposed Explicit and Unconditionally Stable FDTD Method

Based on the aforementioned root-cause analysis, the essential idea of this paper to make an explicit FDTD unconditionally stable is to remove the eigenmodes of $\mathbf{M}$ whose eigenvalues ξ_i do not satisfy (16) instead of choosing a time step Δt to make (16) satisfied for every eigenmode. The latter makes the time step limited by the space step, while the former is free of such a constraint. This is the key difference between the proposed explicit FDTD method and the conventional FDTD method, and why we call the proposed method unconditionally stable. The accuracy of such an approach is guaranteed because the eigenvectors of $\mathbf{M}$ form a complete set of bases for representing the field solution, and the eigenvectors whose eigenvalues violate (16) are not required by accuracy if the time step is chosen based on accuracy, as analyzed in the above section.

For the complete removal of the unstable eigenmodes, we expand the field solution strictly in the space of stable modes, and also project the numerical system onto the same stable space. This is the same as changing the underlying numerical system, namely, matrix $\mathbf{M}$, from the space of all eigenmodes to the space of stable modes only, and then performing an explicit marching strictly in the stable space. It is very important to change $\mathbf{M}$ because $\mathbf{M}$ resulting from space discretization is the source of the unstable modes, while the field solution is not. Regardless of how much the solution is cleaned up at each time, the source of instability still exists in the numerical system resulting from space discretization. The numerical round-off error, the source excitation, etc. all can excite the unstable modes inherent in the numerical system when marching from current step to the next step, no matter how much the field solution is free of unstable modes at current step. The proposed method can also be viewed as enlarging the space step without changing the original space discretization, instead, achieving it in the eigenspace.

Following the aforementioned analysis, there are two straightforward steps in the proposed explicit and unconditionally stable FDTD method. First, find the space of stable modes for the given time step; second, perform an explicit marching that is stable for the given time step irrespective of the space step, no matter how large the time step is. In the proposed algorithm, both steps are developed to retain the strength of an explicit FDTD method in avoiding a system matrix solution. As a result, the unconditional stability is achieved without compromising the linear (optimal) complexity of the traditional explicit FDTD method. To help understand the proposed method, in what follows, we will begin with the explicit marching with unconditional stability, assuming the space of stable modes has been found; we then proceed to elaborate a fast linear-complexity algorithm to find the space of stable modes for the given time step regardless of its size.

A. Explicit Marching With Unconditional Stability

The general 3-D electromagnetic problems simulated by the FDTD can be either a closed-region or an open-region problem. For the former, the boundary condition at the truncation boundary is known; while for the latter, an ABC is generally used with the PML being a popular choice. Since the solution in the artificially constructed ABC is fictitious, we only span the field solution inside the solution domain in the space of stable modes, and project the numerical system inside the solution domain onto the space of stable modes, while leaving the FDTD simulation inside ABCs as usual. This is also done in view of the fact that the artificially constructed ABCs such as the PML does not have fine features relative to the working wavelength, and the small time-step issue of an explicit FDTD in general arises from the fine features inside the solution domain. Thus, the $\mathbf{M}$ matrix in (3) is built for the solution domain only.

We divide the unknown E into two groups, one inside the solution domain denoted by E_S, and the other elsewhere such as boundary, PML, or other ABCs denoted by E_O. The same is done for unknown H. Subsequently, the sparse matrices $\mathbf{D}_E$ and $\mathbf{D}_H$ are cast into the following form:

$$\mathbf{D}_E = \begin{bmatrix} \mathbf{D}_{E,SS} & \mathbf{D}_{E,SO} \\ \mathbf{D}_{E,OS} & \mathbf{D}_{E,OO} \end{bmatrix}$$
$$\mathbf{D}_H = \begin{bmatrix} \mathbf{D}_{H,SS} & \mathbf{D}_{H,SO} \\ \mathbf{D}_{H,OS} & \mathbf{D}_{H,OO} \end{bmatrix} \tag{23}$$

With the above, rewriting the first equation in (1) separately for H_S and H_O, we obtain

$$H_S^{n+\frac{1}{2}} = H_S^{n-\frac{1}{2}} - \Delta t \mathbf{D}_{E,SS} E_S^n - \Delta t \mathbf{D}_{E,SO} E_O^n \tag{24}$$
$$H_O^{n+\frac{1}{2}} = H_O^{n-\frac{1}{2}} - \Delta t \mathbf{D}_{E,OO} E_O^n - \Delta t \mathbf{D}_{E,OS} E_S^n. \tag{25}$$

Similarly, we have for the second equation in (1)

$$E_S^{n+1} = E_S^n + \Delta t \mathbf{D}_{H,SS} H_S^{n+\frac{1}{2}} + \Delta t \mathbf{D}_{H,SO} H_O^{n+\frac{1}{2}} + (\Delta t) j^n \tag{26}$$
$$E_O^{n+1} = E_O^n + \Delta t \mathbf{D}_{H,OO} H_O^{n+\frac{1}{2}} + \Delta t \mathbf{D}_{H,OS} H_S^{n+\frac{1}{2}} \tag{27}$$

where current source j is added for problems with sources.

Given a time step Δt, let the space of the stable modes for the given Δt for E be $\mathbf{V}_{E,st}$, and that for H be $\mathbf{V}_{H,st}$. As shown in Section II, $\mathbf{V}_{E,st}$ is nothing but the subset of the eigenvectors of $\mathbf{M}$ whose eigenvalues satisfy (16). The $\mathbf{V}_{H,st}$ has a simple relationship with $\mathbf{V}_{E,st}$ based on (1) or (10) as the following:

$$\mathbf{V}_{H,st} = \mathbf{D}_E \mathbf{V}_{E,st}. \tag{28}$$

We then expand the field solutions inside the solution domain, E_S and H_S, by their stable modes as the following:

$$E_s = \mathbf{V}_{E,st} y_e \quad H_s = \mathbf{V}_{H,st} y_h \tag{29}$$

with y_e and y_h being unknown coefficient vectors. We also orthogonalize $\mathbf{V}_{E,st}$ so that $\mathbf{V}_{E,st}^T \mathbf{V}_{E,st} = \mathbf{I}$.

Substituting (29) into (24), we obtain

$$\mathbf{V}_{H,st} y_h^{n+\frac{1}{2}} = \mathbf{V}_{H,st} y_h^{n-\frac{1}{2}} - \Delta t \mathbf{D}_{E,SS} \mathbf{V}_{E,st} y_e^n - \Delta t \mathbf{D}_{E,SO} E_O^n. \tag{30}$$

Similarly, substituting (29) into (26) and multiplying both sides of (20) by $\mathbf{V}_{E,st}^T$, we obtain

$$y_e^{n+1} = y_e^n + \Delta t \mathbf{V}_{E,st}^T \mathbf{D}_{H,SS} \mathbf{V}_{H,st} y_h^{n+\frac{1}{2}} + \Delta t \mathbf{V}_{E,st}^T \mathbf{D}_{H,SO} H_O^{n+\frac{1}{2}} + \Delta t \mathbf{V}_{E,st}^T j^n. \tag{31}$$

To facilitate efficient computation, we further simplify the above equations (30) and (31) as follows. Multiplying $\mathbf{V}_E^T \mathbf{D}_{H,SS}$ on both sides of (30), and utilizing the identity of

$$\mathbf{V}_{E,st}^T \mathbf{D}_{H,SS} \mathbf{V}_{H,st} = \mathbf{V}_{E,st}^T \mathbf{D}_{H,SS} \mathbf{D}_{E,SS} \mathbf{V}_{E,st} = \mathbf{V}_{E,st}^T \mathbf{M} \mathbf{V}_{E,st} = \mathbf{\Lambda}_{st} \tag{32}$$

where $\mathbf{\Lambda}_{st}$ is the diagonal matrix consisting of the eigenvalues of $\mathbf{M}$ satisfying (16), we obtain

$$y_h^{n+\frac{1}{2}} = y_h^{n-\frac{1}{2}} - \Delta t y_e^n - \Delta t \mathbf{\Lambda}_{st}^{-1} \mathbf{V}_{E,st}^T \mathbf{D}_{H,SS} \mathbf{D}_{E,SO} E_O^n. \tag{33}$$

Utilizing (32), (31) can also be simplified to

$$y_e^{n+1} = y_e^n + \Delta t \mathbf{\Lambda}_{st} y_h^{n+\frac{1}{2}} + \Delta t \mathbf{V}_{E,st}^T \mathbf{D}_{H,SO} H_O^{n+1/2} + \Delta t \mathbf{V}_{E,st}^T j^n. \tag{34}$$

Since $\mathbf{M}$ has a null space, the smallest eigenvalue is zero. For this eigenvalue, (33) appears to be singular. However, since the null-space modes of $\mathbf{M}$ have a zero curl, the corresponding H is zero. Thus, we only need to set the entries of vector y_h corresponding to zero eigenvalues to be zero.

Both (33) and (34) do not require matrix solutions since the matrix associated with the most advanced time step is identity. This matrix is the left-hand-side matrix in front of $y_h^{n+\frac{1}{2}}$ in (33), and the left-hand-side matrix in front of y_e^{n+1} in (34). Thus, the matrix-free merit of the traditional explicit FDTD is preserved. Furthermore, since $\mathbf{\Lambda}_{st}$ is diagonal, the computation of the right-hand sides of (33) and (34) only requires a few matrix-vector multiplications. More important, unlike the traditional explicit FDTD, (33) and (34) are stable for the given time step irrespective of its size. After the unknown coefficient vectors y_e and y_h are found from (33) and (34), the entire field solution can be reconstructed at any selected point of interest from (29).

B. Proposed Linear-Complexity Algorithm for Finding the Space of Stable Modes for Any Given Time Step

The space of stable modes $\mathbf{V}_{E,st}$ can be directly constructed from the eigenvectors of $\mathbf{M}$, whose eigenvalues satisfy (16). However, the computational efficiency of such an approach may not be desirable when the size of $\mathbf{M}$ is large. We hence develop the following fast linear-complexity algorithm to find $\mathbf{V}_{E,st}$ efficiently. In this algorithm, we keep the advantage of the conventional FDTD in being free of matrix solutions. Meanwhile, we do not suffer from the shortcomings of the conventional FDTD when the time step is small since we only need to perform the traditional FDTD time marching in a small time window to identify stable modes instead of finishing the entire simulation.

In the proposed algorithm, we start the conventional FDTD simulation of (24)–(27). At selected time instants such as at every pth step ($p \geq 1$, a good choice is the ratio of time step required by accuracy to the time step determined by stability) or adaptively determined time instants, we perform three subtasks as follows.

1) Add E field solution E_S in matrix $\mathbf{F}_E$ (initialized to be zero) as a column vector, and also orthogonalize $\mathbf{F}_E$ to ensure the newly added solution vector E_S is not linearly dependent on the solution vectors that are present in $\mathbf{F}_E$. The column dimension of $\mathbf{F}_E$ after orthogonalization is denoted by k' and its row dimension, i.e., the length of E_S, is denoted by N_e.
2) With $\mathbf{F}_E$, we transform the original $\mathbf{M}$ in the solution domain to a reduced $\mathbf{M}_r$ as the following:
$$\underbrace{\mathbf{M}_r}_{k' \times k'} = \underbrace{\mathbf{F}_E}_{k' \times Ne}{}^T \mathbf{D}_{H,SS} \mathbf{D}_{E,SS} \underbrace{\mathbf{F}_E}_{Ne \times k'} \tag{35}$$
which can be obtained in linear complexity $O(N_e)$ by performing computation in sequence from right to left.
3) We compute the eigenvalues and eigenvectors of $\mathbf{M}_r$. Since the size of $\mathbf{M}_r$, k' is small, its eigenvalue solution can be obtained with negligible cost.

To adaptively determine the time instants to perform the aforementioned three subtasks, one can check whether the new field solution obtained, E_S, contains new information that has not been covered by $\mathbf{F}_E$ or not. This can be quantitatively assessed by $\left\| E_S - \mathbf{F}_E \mathbf{F}_E^T E_S \right\| / \| E_S \|$. If this number is smaller than a prescribed tolerance, we do not perform the aforementioned three subtasks; otherwise, we do.

When progressively adding a solution vector into $\mathbf{F}_E$ in the above process, repeating eigenvalues will be observed from the eigenvalue solution of the reduced matrix (35). These repeating eigenvalues, when the weights of their eigenvectors become dominant in the field solution, correspond to the physically important eigenvalues of the original system as analyzed in [13] (the physically important eigenvalues are the eigenvalues of $\mathbf{M}$, whose corresponding eigenvectors have a non-negligible weight in the E-field solution). Based on this fact, the aforementioned time-marching procedure for identifying stable modes can be terminated when the following two criteria are satisfied.

First, the weights of the eigenmodes of $\mathbf{M}_r$ corresponding to the repeating eigenvalues become dominant as compared to the weights of other eigenmodes based on accuracy criterion ε_1. Denoting the eigenmodes of $\mathbf{M}_r$ corresponding to the repeating eigenvalues by $\mathbf{V}_{r,l}$, and the other eigenmodes by $\mathbf{V}_{r,h}$. Their weights y_{el} and y_{eh} can be determined from

$$y_{el} = \mathbf{V}_{r,l}^T \mathbf{F}_E^T E_S(t) \quad y_{eh} = \mathbf{V}_{r,h}^T \mathbf{F}_E^T E_S(t). \tag{36}$$

In arriving at the above equations, we utilize the fact that $\mathbf{F}_E$ is orthogonal and so are the eigenvectors of $\mathbf{M}_r$. The dominance of the $\mathbf{V}_{r,l}$ is assessed by

$$\frac{\left|y_{eh}^T y_{eh}\right|}{\left|y_{el}^T y_{el}\right|} \leq \varepsilon_1. \tag{37}$$

The second criterion is to examine whether the difference between the repeating eigenvalues identified at adjacent steps is smaller than a prescribed error tolerance ε_2, which is written as

$$\frac{\left|\xi_{i,l}^{(j+1)} - \xi_{i,l}^{(j)}\right|}{\left|\xi_{i,l}^{(j)}\right|} \leq \varepsilon_2 \tag{38}$$

where $\xi_{i,l}^{(j)}$ denotes a repeating eigenvalue at the jth step. The smaller the ε_1 and ε_2 are, the better the accuracy. However, the simulation will also take longer time. In general, the choice of $1\mathrm{e}{-3}$ or $1\mathrm{e}{-4}$ is sufficient to produce a good level of accuracy without sacrificing efficiency.

When both conditions, (37) and (38), are satisfied, a complete and accurate set of physically important eigenmodes of the original system is found from which we select the eigenvectors of reduced matrix $\mathbf{M}_r$ whose eigenvalues satisfy (16) to form $\mathbf{V}_{r,st}$ that is stable and accurate for the given time step. $\mathbf{V}_{E,st}$ can then be obtained from

$$\underbrace{\mathbf{V}_{E,st}}_{Ne\times k} = \underbrace{\mathbf{F}_E}_{Ne\times k'}\ \underbrace{\mathbf{V}_{r,st}}_{k'\times k} \tag{39}$$

where k denotes the number of stable modes. The above is then used in (33) and (34) to perform explicit time marching. Notice that we do not have to multiply $\mathbf{F}_E$ and $\mathbf{V}_{r,st}$ together to construct $\mathbf{V}_{E,st}$, we only need the expression of (39) since only matrix-vector multiplications are needed in (33) and (34). The eigenvalues contained in the diagonal matrix $\mathbf{\Lambda}_{st}$ in (33) and (34) are also known from the repeating eigenvalues corresponding to the stable modes identified in the aforementioned procedure.

IV. Complexity and Accuracy Analysis

A. Complexity Analysis

The overall procedure of the proposed method and the complexity of each step are summarized as follows.

Step I: A preprocessing step to find the space of stable modes for the given time step irrespective of its size, which is performed based on the algorithm described in Section III-B.

(I-1): Perform the conventional explicit FDTD simulation of (1) and march on in time by one step. The complexity is linear $O(N)$, where N is the total number of electric and magnetic field unknowns.

(I-2): At selected time instants, the number of which is $O(k)$, perform the following four subtasks.

(a) Add $\mathbf{E}$ field solution vector E_S as a column vector in $\mathbf{F}_E$, and orthogonalize it with respect to the other vectors in $\mathbf{F}_E$. The complexity is $k'O(N_e)$, which is linear.

(b) Construct a reduced matrix $\mathbf{M}_r$ shown in (35), the complexity of which is $k'O(N_e)$. Notice that we only need to compute the blocks associated with the newly added column vector in $\mathbf{F}_E$ since the other block in $\mathbf{M}_r$ is known from the computation at previous steps.

(c) Solve a reduced eigenvalue problem of size k' for $\mathbf{M}_r$, the cost of which is negligible because of the reduced matrix size.

(d) Check the weights of different eigenmodes in the field solution from (36). The operation count is $k'O(N_e)$. Examine whether (37) and (38) are satisfied. If not satisfied, we go back to Step (I-1); if satisfied, we stop. The space of stable modes, (39), is completed.

Step II: Explicit time marching stable for any given time step.

(II-1) Perform time marching in a reduced space of stable modes. Compute unknown coefficient vectors y_e and y_h from (33) and (34). The cost is $O(k)$ if no artificial absorber exists, where k is the number of stable modes. If there is an artificial absorber such as a PML, the computational complexity is $k\mathrm{O}(N_B)$ at each time, where N_B is the number of unknowns at the interface between the solution domain and the artificial absorber, which is much smaller than N. The FDTD marching inside the artificial absorber is performed as usual, the complexity of which is linear.

(II-2) After y_e and y_h are obtained at all time steps, the field solution can be readily constructed from (29) at each time instant since $\mathbf{V}_{E,st}$ and $\mathbf{V}_{H,st}$ are time independent. Same as [13], if only m selected solutions are needed, we can select the m rows to compute E and H, the cost is $O(m)$.

In summary, the linear complexity of the original explicit FDTD at each time step without solving a matrix equation is retained in the proposed method, while the shortcoming of the conventional FDTD in stability is overcome.

B. Accuracy Analysis

If the time step is chosen based on accuracy, the space of stable eigenmodes, $\mathbf{V}_{E,st}$, for the given time step is also the accurate space to represent the field solution at any time instant. In other words, (29) is an accurate representation of the electric and magnetic fields. To explain, from (18), field solution E at any frequency for an arbitrary source $\tilde{j}$ can be written as [13]

$$\begin{aligned} E(\omega) &= \mathbf{V}_E(\Lambda - \omega^2\mathbf{I})^{-1}\mathbf{V}_E^T\tilde{j} \\ &= \mathbf{V}_{E,st}\tilde{y}_e + \mathbf{V}_{E,\mathrm{unstable}}\tilde{y}_{e,\mathrm{unstable}} \end{aligned} \tag{40}$$

where Λ is the diagonal matrix composed of the eigenvalues of $\mathbf{M}(\xi_i)$, and eigenvector matrix $\mathbf{V}_E$ is split into two groups, stable modes $\mathbf{V}_{E,st}$ whose eigenvalues satisfy (16), and unstable ones $\mathbf{V}_{E,\mathrm{unstable}}$ whose eigenvalues violate (16). It is evident from (40) that the weight of each eigenmode in field solution is proportional to $(\xi_i - \omega^2)^{-1}$. The larger the eigenvalue as compared to ω^2, the smaller the contribution of its corresponding eigenvector to the field solution. Therefore, given an input spectrum and a required accuracy, there is a maximum ξ_i to be kept in the field solution, the corresponding frequency of which is denoted by $f_{\max}$. Eigenmodes whose eigenvalues are greater than such a maximum value can be removed without sacrificing the prescribed accuracy since their weights in the field solution are negligible. When the time step is chosen based on accuracy, the eigenvalues of the unstable modes are

beyond the maximum frequency required by accuracy, as can be seen from (22). Hence, the unstable component in (40) can be eliminated without sacrificing the required accuracy, leaving the stable modes $\mathbf{V}_{E,st}$ an accurate space to represent field solutions at any frequency and any time.

V. Numerical Results

We first demonstrate the unconditional stability of the proposed method. We then simulate a number of 2-D and 3-D examples in both open- and closed-region settings to examine the accuracy, efficiency, and stability of the proposed method in comparison with the traditional explicit FDTD method.

A. Demonstration of Unconditional Stability

We simulate a 3-D parallel-plate structure whose analytical solution is known. The material is air in between the plates. The structure has a 1-μm height (along z), 6-μm width (along y), and 900-μm length (along x). The space step is 0.333, 0.85417, and 90 μm, respectively, along the z-, y-, and x-direction. A vertical current source is injected at the near end of the parallel-plate structure from the bottom plate to top plate. The voltage waveforms are sampled at both near and far ends. The computational domain is truncated by a perfect electric conductor (PEC) boundary condition at the bottom and on the top, and by perfect magnetic conductor (PMC) boundary condition elsewhere. The waveform of the current source is a Gaussian derivative pulse of $I(t) = 2(t-t_0)e^{-((t-t_0)/\tau)^2}$ with $\tau = 0.2$ s and $t_0 = 4\tau$. Due to the small space step of the structure, the traditional FDTD must use a time step as small as 1.0363×10^{-15} s in order to maintain the stability of time-domain simulation. In contrast, for the same space step, the proposed method can use an arbitrarily large time step without becoming unstable. For example, to use $\Delta t = \infty$, we only need to keep zero-eigenvalue modes in (29) while discarding others. The voltages generated from the proposed method with a time step of 0.001, 0.01, and 0.1 s are, respectively, shown in Fig. 1, while with the same time step, the conventional FDTD simply diverges. In addition, the results generated with a time step of 0.01 and 0.001 s are not only stable, but also accurate since the time step of 0.01 and 0.001 s satisfies accuracy requirements for the given input spectrum. This can be clearly seen from the excellent agreement between the solutions generated from the proposed method and analytical solution, as shown in Fig. 1. Thus, with a time step 10^{13} times larger than that permitted by the CFL condition, the proposed method still generates both stable and accurate results.

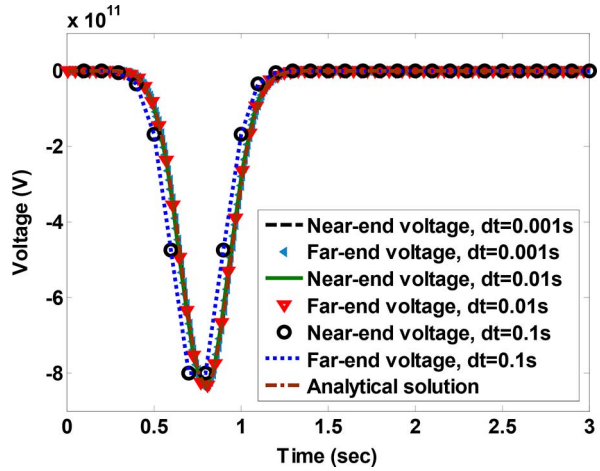

Fig. 1. Voltages of an μm-level 3-D structure simulated with different time steps in comparison with an analytical solution.

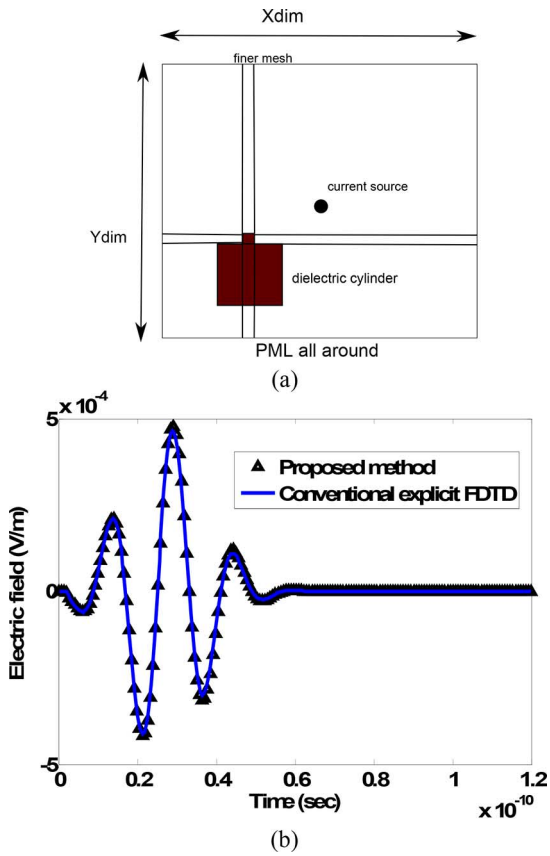

Fig. 2. Simulation of a 2-D dielectric cylinder with a fine feature in the presence of a current source. (a) Problem setup ($X\text{dim} = Y\text{dim} = 2.1$ mm). (b) Electric field solution.

B. Demonstration of Accuracy, Efficiency, and Stability

1) 2-D Dielectric Cylinder Scattering: A 2-D dielectric cylinder comparable to wavelength with a fine notch, as shown in Fig. 2(a), is simulated in the presence of a line current source. The current source is placed at the center of a solution domain of dimension 2.1 mm $\times$ 2.1 mm, the waveform of which is $I(t) = \exp(-0.5(t-t_0)^2/\tau^2)\sin(2\pi ft)$ with $t_0 = 2.5 \times 10^{-11}$ s, $\tau = 1.0407 \times 10^{-11}$s, and $f = 60$ GHz. The solution domain is truncated by a PML region, which has five grid cells all around the solution domain with a uniform cell size of 71.43 μm. The width and height of the dielectric notch are both 3.57 μm, and the side length of the square cylinder is 357.15 μm. To capture the fine feature of the notch, a non-uniform grid is used, with the smallest grid size being 3.57 μm and the largest one being 71.43 μm. The region of the dielectric cylinder and the notch is occupied by a material having $\mu_r = 1$ and $\varepsilon_r = 2$.

The electric field sampled at the center of the right-most boundary is plotted in Fig. 2(b) and compared with the result from a conventional FDTD method. We observe excellent agreement. In addition to correlating results at randomly selected points, we have also assessed the *entire* solution error of the proposed method by evaluating $\|u - u_{\text{ref}}\|/\|u_{\text{ref}}\|$, where

vector u contains all the unknown electric and magnetic fields in the solution domain computed from the proposed method, whereas $u_{\rm ref}$ is the reference solution obtained from (33) and (34) with all eigenmodes of $\mathbf{M}$ included and computed directly from the $\mathbf{M}$'s eigenvalue solution. The maximum error of the proposed method at all time is shown to be 0.88%, verifying the accuracy of the proposed method.

To simulate this example, the time step for a conventional FDTD simulation is 2.671×10^{-15} s. In contrast, the proposed method is able to use a time step of 1.3065×10^{-13} s solely determined by accuracy to perform the time-domain simulation. The total CPU time cost by a traditional FDTD is 7068.5 s, whereas the time of the proposed method is 217.8 s including the CPU time of both the preprocessing and the unconditionally stable time marching. Among the 217.8 s, the time cost by the traditional FDTD marching in the pre-processing step is 204.3567 s [the cumulative time of Step (I-1)], the time cost by the identification of physically important eigenmodes including the computation of the small eigenvalue problem is 0.2135 s [the cumulative time of Step (I-2)], and the time cost in the explicit time-marching in Step II is 13.2392 s. Comparing the 204.3567 s cost by the proposed method in Step (I-1) with the total 7068.5 s cost by the traditional FDTD, it is evident that only a small time window needs to be simulated to identify all the physically important eigenmodes. The ε_1 and ε_2 chosen in the proposed method are 10^{-4}, and 10^{-5}, respectively; and the number of steps to collect FDTD solutions, p, is five. Twenty physically important eigenmodes have been identified from the preprocessing procedure, whose square roots of eigenvalues are 0.0916e+13, 0.2081e+13, 0.2980e+13, 0.3779e+13, 0.4489e+13, 0.4664e+13, 0.5327e+13, 0.5971e+13, 0.6571e+13, 0.7058e+13, 0.7709e+13, 0.8177e+13, 0.8766e+13, 0.9578e+13, 0.9816e+13, 1.0594e+13, 1.0934e+13, 1.1304e+13, 1.1842e+13, and 1.1870e+13, respectively. Notice that any nonzero eigenvalue of $\mathbf{M}$ corresponds to a full-wave field distribution since the corresponding eigenvector does not satisfy curl $\mathbf{E}$ equal to zero since $\mathbf{M}V_{E,i}$ is not zero.

We then shrink the size of the dielectric notch to 35.7 nm. The proposed method takes 1.3252×10^{3} s to finish the entire simulation while the conventional FDTD costs 1.067×10^{6} s, yielding a speedup of more than 805. The time step of the proposed method is 1.3065×10^{-13} s, whereas that of the traditional FDTD is 1.899×10^{-16} s. The difference between the entire solution computed from the proposed method and that of the conventional FDTD is assessed by $\|u - u_{\rm FDTD}\|/\|u_{\rm FDTD}\|$ at all time, the maximum of which is shown to be less than 1.4%. The 2-norm is used to compute the vector norm.

2) Dipole Antenna Radiation in 3-D Free Space: The second example is the radiation of a dipole antenna in 3-D free space. The dipole of length 300 μm is placed at the center of a solution domain of dimension 900 μm $\times$ 600 μm $\times$ 300 μm. The source waveform is a fast Gaussian derivative pulse with $\tau = 3\times10^{-11}$ s, and $t_0 = 4\tau = 12\times10^{-11}$ s. The solution domain is truncated by a PML region that has 20 grid cells all around the solution domain with a uniform cell size of 100, 85.714, and 60 μm in x-, $y-$, and z-direction, respectively. The electric field sampled at the center of the right-most boundary is plotted in Fig. 3 and

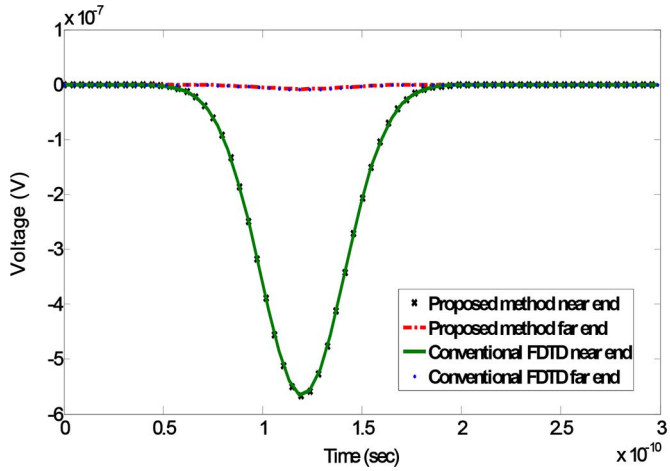

Fig. 3. Simulation of the radiation of a dipole in 3-D free space.

compared with the result from a conventional FDTD method, which reveals an excellent agreement. Such an agreement is not only observed at randomly selected points, but also in the entire solution vector. The maximum difference between the proposed solution and the conventional FDTD solution, measured by $\|u - u_{\rm FDTD}\|/\|u_{\rm FDTD}\|$ at all time, is shown to be less than 0.43%. The time step is 1.4714×10^{-13} s to maintain the stability of a conventional FDTD simulation. Since there is no fine feature involved in this example, the space step is chosen solely based on accuracy, thus the time step required by accuracy is also at the level of 1.4714×10^{-13} s. In this example, since the problem size is small, we directly compute the eigensolution of the $\mathbf{M}$ matrix to build the space of stable modes. The total time cost by a traditional FDTD is 294 s, whereas the time of the proposed method is 254 s, although the same time step is used. This is due to the reduced system size in the step of unconditionally stable explicit marching, where the solution is found in a reduced space of stable modes.

3) 3-D Parallel-Plate Waveguide: The third example is the 3-D parallel-plate structure simulated in Section V-A, but with a fast Gaussian derivative pulse having a maximum input frequency of 34 GHz, at which the spectrum decays to 10^{-3} of its maximum value. To simulate this example, a conventional explicit FDTD method requires a time step as small as 1.0363×10^{-15} s to maintain the stability of the time-domain simulation because the smallest space step is 0.33 μm. In contrast, the proposed explicit method is able to use a large time step of 1.1928×10^{-12} s based on accuracy to generate accurate and stable results. As shown in Fig. 4, the voltage waveforms simulated by the proposed method agree very well with those generated by the conventional explicit FDTD. This agreement is not only observed at selected points, but also in the entire solution vector. The maximum difference between the proposed solution and the conventional FDTD solution, measured by $\|u - u_{\rm FDTD}\|/\|u_{\rm FDTD}\|$ at all time, is shown to be less than 1.37%. It is worth mentioning that this does not mean the proposed method is less accurate than the conventional FDTD by 1.37%. This only shows that the two methods are different by 1.37%. To clarify, we have compared both the proposed method with the "golden reference" that is obtained by solving the eigenvalue problem of $\mathbf{M}$ as it is and march on in time with (33) and

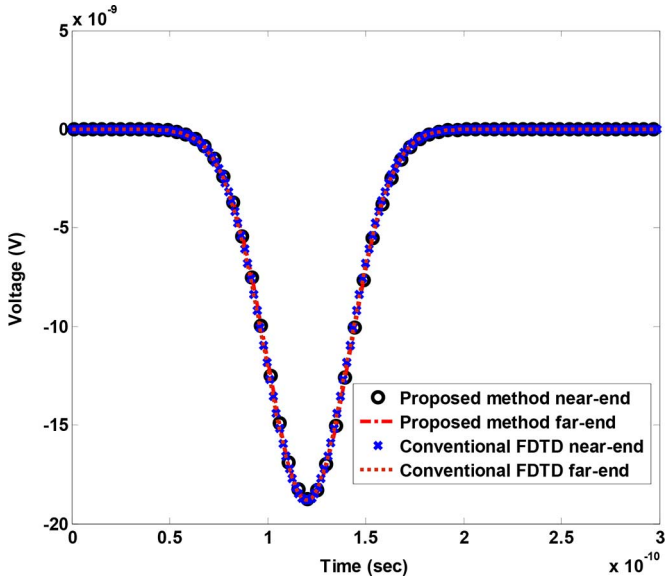

Fig. 4. Simulation of a 3-D parallel plate structure.

(34) using all eigenvectors of $\mathbf{M}$ without any removal. Since the space dependence of the field solution in this approach is obtained without time marching and approximation, its accuracy in space dependence is not degraded by time stepping. Let this solution be $u_{\rm ref}$, we find $\|u-u_{\rm ref}\|/\|u_{\rm ref}\|$ to be 0.65%, while $\|u_{\rm FDTD}-u_{\rm ref}\|/\|u_{\rm ref}\|$ is 0.76%.

Since the problem size is small, the full eigensolution of the $\mathbf{M}$ matrix is computed to build the space of stable modes. The total time required by the proposed method is approximately 11 s. Compared with 12419.7109 s required by the conventional explicit FDTD, the proposed method has a speedup of 1164. The ε_1 and ε_2 chosen in the proposed method are 10^{-3}, and 10^{-5}, respectively. The solutions are sampled every 50 steps in the preprocessing. Two physically important eigenmodes are identified from the preprocessing procedure, whose square roots of eigenvalues are zero, and 5.2710e+11, respectively.

4) 3-D On-Chip Bus Structure: The fourth example is an on-chip 3-D bus structure, as shown in Fig. 5(a). The width of each bus is 3 μm and so is the spacing between buses. The buses are in the stack of four dielectric layers. The structure is excited with two current sources, one is from bus 1 to bus 2 and the other is from bus 3 to bus 2. The type of current sources is the same as that in Section V-B.3). The number of cells along the x-direction is ten, along the y-direction is eight, and along the z-direction is five. Thus, the space step along the x-direction is 50 μm, along the y-direction is 1.875 μm, and along the z-direction is 0.3 μm. The ε_1 and ε_2 chosen in the proposed method are 10^{-3}, and 10^{-5}, respectively. The solutions are sampled every 50 steps in the preprocessing. Seven physically important eigenmodes are identified from the preprocessing procedure, whose square roots of eigenvalues are 0.0, 0.8084e+11, 0.8558e+11, 0.9239e+11, 1.6006e+11, 1.6903e+11, and 1.853e+11, respectively.

In the conventional FDTD, the time step, constrained by the smallest space step, is 9.9355×10^{-16} s. In contrast, the time step in the proposed method solely determined by accuracy regardless of space step is 5.3928×10^{-13} s. For this time step, the total CPU time of the proposed method is 261.2 s, whereas the total time of the conventional FDTD is 11951.1 s, yielding

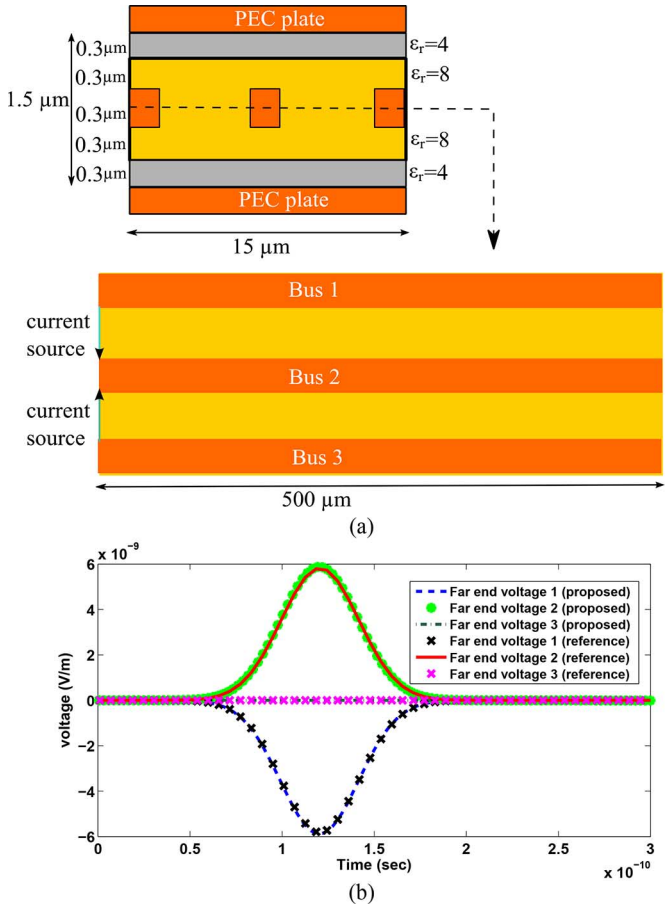

Fig. 5. Simulation of a 3-D on-chip bus structure. (a) Structure. (b) Voltage waveforms.

a speedup of approximate 47. In the total time cost by the proposed method, the time cost by the traditional FDTD marching in the preprocessing step is 255.9 s (the cumulative time of Step (I-1) in the preprocessing step), the cumulative time of Step (I-2) in the preprocessing step is 0.5057 s, and the time cost in the explicit time-marching in Step II is 4.8 s. In Fig. 5(b), the voltages sampled at the far end between bus 1 and bus 2, bus 2 and bus 3, and bus 1 and bus 3 obtained from the proposed method are compared with those obtained from the conventional FDTD method. The maximum difference between the proposed solution and the conventional FDTD solution, measured by $\|u-u_{\rm FDTD}\|/\|u_{\rm FDTD}\|$ containing all field solutions at all time, is shown to be less than 2.6%. We have also correlated both the proposed method and the conventional FDTD with the "golden reference" solution $u_{\rm ref}$. The $\|u-u_{\rm ref}\|/\|u_{\rm ref}\|$ is found to be 0.75%, whereas $\|u_{\rm FDTD}-u_{\rm ref}\|/\|u_{\rm ref}\|$ is 2.1%.

5) Large-Scale Example: Phantom Head Beside a Wire Antenna: With the accuracy and efficiency of the proposed method validated, we applied the method to a large-scale phantom head example [17] with over 48 million unknowns, which cannot be simulated by the conventional FDTD in a feasible run time due to the existence of fine tissues relative to the working wavelength, whose corresponding frequency is 1.8 GHz. The maximum dielectric constant is 67.636, and the average one is 9.9. The dimension of the phantom head is 28.16 cm $\times$ 28.16 cm $\times$ 17.92 cm, whose largest size is over five wavelengths. The number of discretization cells in

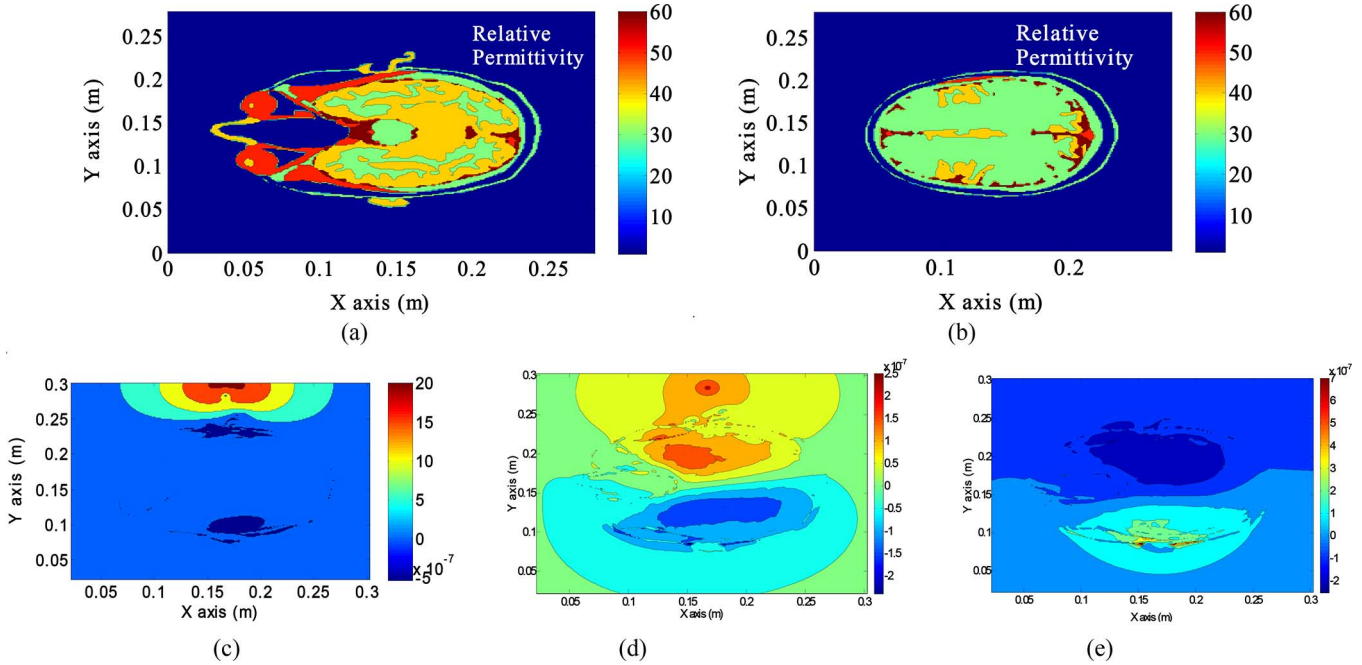

Fig. 6. Simulation of a phantom head beside a wire antenna. (a) and (b) Relative permittivity in a cross section at a height of 11.2 and 5.6 cm. (c)–(e) Electric field distribution at three different time instants in a cross section at a height of 11.2 cm.

the solution domain is $255 \times 255 \times 127$, while the number of cells used in the PML is 20 in each direction. Thus, the total number of cells is $295 \times 295 \times 167$. The smallest space step in the x-, y-, and z-direction are, respectively, 0.011, 1.1, and 1.4 mm. The input current source has a waveform of Gaussian derivative, located at $x = 14.52$ cm and $y = 26.18$ cm. To maintain stability, the traditional FDTD requires a time step of 7.3378×10^{-14} s. The proposed method is able to use a time step of 4.5360×10^{-12} s solely determined by accuracy regardless of space step. Fifteen stable modes are identified from the preprocessing procedure with the choice of $p = 58$, $\varepsilon_1 = 10^{-2}$, and $\varepsilon_2 = 10^{-4}$, the smallest six eigenvalues of which are, respectively, 0, 4.54615e+20, 2.67124e+21, 3.88910e+22, 4.50825e+22, and 4.86821e+22. The total CPU time cost by the traditional FDTD is 3.3779e5 s (projected based on the time cost at each step), whereas the total CPU time of the proposed method including both preprocessing and explicit time marching is only 8858 s, thus a speedup of 38. In the total time cost by the proposed method, the time cost by the traditional FDTD marching in the pre-processing step is 7663.2 s [the cumulative time of Step (I-1)], the cumulative time of Step (I-2) is 0.0216 s for computing a small eigenvalue problem and identifying physically important eigenmodes, and the time cost in Step II is 1194.8 s for explicit time marching. The total number of time steps simulated in the preprocessing step is 3538, rendering a small time window of $2.596e{-}10$ s. The relative permittivity distribution is shown in Fig. 6(a), and (b), respectively, at the height of 11.2 and 5.6 cm. The contour plots of the z-component electric field at three different time instants in a cross section at a height of 11.2 cm are shown in Fig. 6(c)–(e).

All of the aforementioned examples have been simulated to very late time, no late-time instability has been observed, which is theoretically guaranteed by the proposed method since the numerical system has already been transformed to a new one that is stable for the given time step regardless of how large the time step is.

6) Problems Without Fine Features Relative to Working Wavelength: In the previous examples, some structures are sizable compared to wavelength such as the last 3-D phantom head example and the 2-D dielectric scattering example in Section V-B.1), while others are electrically small. However, all these structures involve fine features relative to the working wavelength. It is also understood that only in these structures there exists a gap between the time step required by accuracy and the time step determined by stability, and hence there is a need for increasing the time step. In this section, to further examine whether the performance of the proposed method relies on fine features or not, we simulate a cavity problem of five wavelengths without any spatially over-resolved features.

The cavity is of dimension 43.2 mm × 34.4 mm × 8.8 mm. The cell size along each of x-, y-, and z-directions is 0.1 wavelength (0.88235 mm). A z-orientated current dipole of one cell size is located at the center of the PEC cavity. Since there are no fine features relative to working wavelength in this structure, the time step for conventional FDTD and that for the proposed method is both 1.6993×10^{-12} s, which is the same as the time step required by accuracy. The waveform of the current pulse is $(1 - e^{-t/d})\sin(2\pi \times 34 \times 10^9 t)$, where d is twice that of the time step. The simulation parameters in the preprocessing step are chosen as $p = 2$, $\varepsilon_1 = 10^{-2}$ and $\varepsilon_2 = 10^{-5}$. The total number of physically important eigenmodes identified in the preprocessing step is 259.

The CPU time of the conventional FDTD is 2465.9 s, whereas the total CPU time of the proposed method is 826 s, yielding a speedup of approximately 3. Among the 826 s, the cumulative time of Step (I-1) is 796.3638 s; the cumulative time of Step (I-2) is 4.558 s; while the time cost in the explicit marching in the

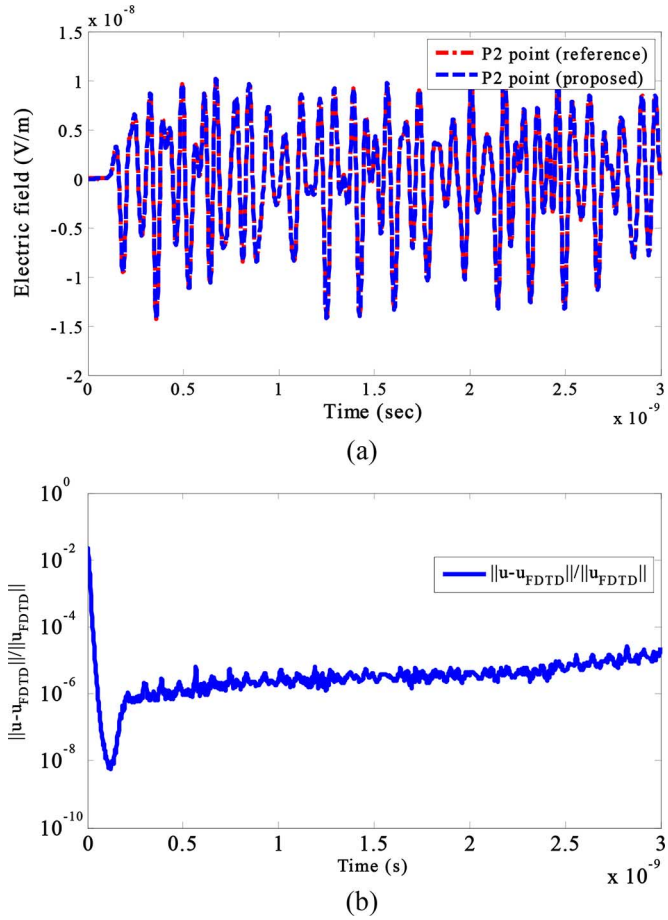

Fig. 7. Simulation of a five-wavelength 3-D cavity without fine features. (a) Comparison with reference solution generated by traditional FDTD at one observation point. (b) Comparison at all points and all time with error evaluated by $\|u - u_{\mathrm{FDTD}}\|/\|u_{\mathrm{FDTD}}\|$.

second step is 25.1393 s. It is evident that even though the structure does not involve spatially over-resolved features, the proposed method has a speedup over the traditional FDTD method. A detailed theoretical analysis will be given in Section V.

The time-domain waveform sampled at a point (42.4, 16.8, and 4.4 mm) is shown in Fig. 7(a) as compared to the result from the conventional FDTD. Excellent agreement is observed. We have also evaluated the total solution error at all time and all points in comparison with the FDTD results by computing $\|u - u_{\mathrm{FDTD}}\|/\|u_{\mathrm{FDTD}}\|$. In Fig. 7(b), we plot such an error versus time. The average error across the whole time window is shown to be $5.165\mathrm{e}{-5}$.

VI. Discussions

In this section, we discuss a few important issues relating to the computational efficiency of the proposed method and the terminology used to describe the proposed method.

1) On the Number of Stable Eigenmodes: The set of the stable eigenmodes for the time step chosen based on accuracy is the set of physically important eigenmodes. These modes are defined as the eigenmodes that cannot be neglected in the field solution for a prescribed accuracy. In [21] and [22], it is shown that the number of physically important eigenmodes required to represent the solution of electrodynamic Maxwell's equations in a general 3-D problem, for any prescribed accuracy and at any frequency, scales *linearly* with the electric size of the problem. In the volume-discretization-based FDTD, the number of unknowns scales *cubically* with the electric size of the problem since each wavelength is discretized into a constant number of points such as ten or others, and there are three dimensions to discretize. Therefore, the number of important eigenmodes k, the upper bound of which is $O(N^{1/3})$ for any frequency, is always much smaller than the unknown size N. For electrically small problems, the k is even a constant irrespective of N for achieving any desired order of accuracy.

In addition to the fact that k is orders of magnitude smaller than N, these k modes can also be extracted band by band in the proposed method. For example, if we encounter a broad frequency band where many eigenmodes are important, we can divide this band into multiple small bands, launch a pulse for each sub-band, and extract the few modes in each sub-band. The union of the eigenmodes in each sub-band is the set of the eigenmodes important for the whole frequency band.

In addition, we do not need to store these eigenmodes as a whole either. Once a set of eigenmodes is found for each sub-band, their contributions to the field solution can already be found by performing Step II in the proposed method. The final field solution is simply the addition of the contribution from each eigenmode. By doing so, the memory we need is just the memory required to store the eigenmodes in each sub-band.

It is also worth mentioning that the stable modes found in this work are frequency and time independent. The non-dc stable modes are also right-hand-side independent. Once found, they can be reused for all simulations. In other words, the preprocessing step in the proposed method can be done once for all simulations.

2) On the Model-Order Reduction (MOR): Although the objective of this paper is to find the root cause of instability, and subsequently remove this root cause in an explicit FDTD method, since the number of stable eigenmodes is smaller than the original system size, as an added bonus, the proposed method also effectively reduces the system order. However, this does not mean a MOR technique alone can solve the stability problem. With a MOR technique, one can solve a reduced-order system to find the solution of the original large problem. However, the stability problem still exists in the reduced order system.

In addition, from the perspective of the MOR, the proposed method is different from existing MOR methods, and offers features that are generally not available in other methods. It generates a minimal-order model [25] required by accuracy; it has a closed-form error bound; the model generation has linear (optimal) complexity (the algorithm of the proposed preprocessing step has linear complexity); and the resultant model-based simulation has a diagonal system.

3) On the Speedup of the Proposed Method: In general, the optimal speedup of an unconditionally stable method over a conditionally stable method without sacrificing accuracy is the ratio of the time step allowed by accuracy (Δt_a) and that permitted by stability (Δt_s). This ratio is the same as the ratio of the space step allowed by accuracy and the actual space step used

in order to capture the fine features relative to working wavelength. If the structure does not involve fine features relative to the working wavelength, then the time step required by stability agrees with that required by accuracy, and then there is no need to enlarge the time step of the FDTD method since that time step is the one needed for accuracy.

In the proposed method, we simulate a time window of width "w" to extract the physically important eigenmodes from the entire structure information contained in $\mathbf{M}$ and the FDTD solutions. Let the total time window to be simulated in the FDTD be T. The speedup of the proposed method is essentially bounded by T/w since after extracting all the physically important eigenmodes and subsequently stable modes for the given time step in the pre-processing step, the explicit FDTD marching is performed on a reduced fully decoupled diagonal system of the stable modes, the time cost of which is negligible as compared to the preprocessing step. Therefore, different from the implicit unconditionally stable methods, the speedup of the proposed method over the traditional FDTD does not have to rely on the spatially resolved features. This has also been numerically verified in the last example in Section V. Certainly, if there are fine features, the speedup over the traditional FDTD can be greater than that without fine features. In addition, by minimizing "w," we can even achieve a more than optimal speedup, as shown in [23].

Numerically, the length of w is adaptively determined through the error control parameters in the proposed preprocessing step instead of artificially assumed. Theoretically speaking, the length of w is shorter than T, i.e., the time we need to simulate to extract the complete set of physically important eigenmodes from $\mathbf{M}$ is always smaller than the time required to finish the entire FDTD simulation regardless of the structure size for the following reason.

As can be seen from (40), which reveals the weight of each eigenmode in the field solution as $(\xi_i-\omega^2)^{-1}$, the contributions to the field solution at a given frequency are dominated by eigenmodes whose eigenvalues are closer to the given frequency. In a time-marching process, the early time response is dominated by the high-frequency components. Therefore, higher order eigenmodes are identified earlier than the low-order modes. Once the lowest physically important eigenvalue is found, our preprocessing step can be terminated since at this time, all the eigenvalues larger than the lowest one should have already been extracted. Therefore, the time window "w" to simulate in the preprocessing step is determined by how soon we can identify the smallest eigenvalue of physical importance. For electrically small problems, the smallest eigenvalue to extract is zero, i.e., dc eigenvalue; for electrically large cases, the smallest eigenvalue to extract is the first nonzero eigenvalue $\xi_{\min}$, whose square root is proportional to $(c\pi)/(l_{\max})$, where $l_{\max}$ denotes the largest problem dimension, and c is the speed of light. Since the weight of each eigenmode in the field solution is proportional to $(\xi_i - \omega^2)^{-1}$, the contribution of a mode whose eigenvalue is ξ_i can already be seen at frequencies higher than $\sqrt{\xi_i}/2\pi$. Therefore, the time "w" we have to simulate can be estimated to be proportional to $1/f$, where f is the highest frequency where the contribution of the $\xi_{\min}$ mode is not negligible, and hence can be detected. Since T is no less than $O(2l_{\max}/c) = O(2\pi/\sqrt{\xi_{\min}})$, while w is $O(1/f)$ and f is larger than $\sqrt{\xi_{\min}}/(2\pi)$, we have w smaller than T. Similar analysis can be done for the electrically small cases.

It is also worth mentioning that the proposed algorithm does not rely on the FDTD marching to traverse the entire structure to sense the structure since the entire structure information is known from space discretization and contained in $\mathbf{M}$. In the proposed algorithm, we extract eigenmodes not just from field solutions, but from both $\mathbf{M}$ and field solutions. The solutions we collect in $\mathbf{F}_E$ are simply used to test the physically important eigenmodes out from the $\mathbf{M}$ matrix. As long as $\mathbf{F}_E$ has a nonzero projection on the physically important eigenmodes, these modes can be found from $\mathbf{M}_r$. This property of the proposed method can be leveraged to further accelerate the proposed method.

In the future, we will continue to study how to further speed up the proposed method. Other options to remove the root cause of instability in an explicit time-domain method will also be explored. Recently, this work has also been extended to analyze general lossy electromagnetic problems in [24].

4) On the New Term of "Explicit and Unconditionally Stable Method": The existing implicit unconditionally stable methods use a time integration method to remove the dependence of the time step on space step; while the proposed method is very different. It certainly does not belong to the class of commonly understood unconditionally stable methods. However, the method presented here also removes the dependence of time step on space step, which is accomplished by adapting the eigenmodes of the system matrix to remove the root cause of instability. If the time step required by accuracy is infinity, the proposed method also allows one to use an infinitely large time step to perform a stable and accurate time-domain simulation. In addition, every spatial Fourier mode contained in a stable eigenmode is stably simulated. From these perspectives, the proposed method has the same features as an unconditionally stable method. It is hoped that this work can help enrich the literature and broaden the definition of the unconditionally stable methods.

VII. Conclusion

In this paper, the root cause of the instability associated with an explicit FDTD method using a time step beyond stability criterion has been analyzed. Based on the root cause analysis, an explicit and unconditionally stable FDTD method has been developed. The strength of the conventional explicit FDTD is retained in avoiding solving matrix equations while its shortcoming is overcome in the time step's dependence on space step. Hence, the proposed work helps remove a major computational bottleneck associated with the explicit FDTD simulation. The comparison with the conventional explicit FDTD method in both 2-D and 3-D simulations have demonstrated the clear advantage of the proposed explicit and unconditionally stable FDTD method in accuracy, efficiency, and stability. Important issues relating to the computational efficiency and the nature of the proposed method have also been discussed. The general idea of the proposed method can be applied to other time-domain methods that solve first-order Maxwell's equations in time.

REFERENCES

[1] K. S. Yee, "Numerical solution of initial boundary value problems involving Maxwell's equations in isotropic media," *IEEE Trans. Antennas Propag.*, vol. AP-14, no. 5, pp. 302–307, May 1966.

[2] A. Taflove and S. C. Hagness, *Computational Electrodynamics: The Finite-Difference Time-Domain Method*. Boston, MA, USA: Artech House, 2000.

[3] F. Zheng, Z. Chen, and J. Zhang, "A finite-difference time-domain method without the Courant stability conditions," *IEEE Microw. Guided Wave Lett.*, vol. 9, no. 11, pp. 441–443, Nov. 1999.

[4] T. Namiki, "A new FDTD algorithm based on alternating-direction implicit method," *IEEE Trans. Microw. Theory Techn.*, vol. 47, no. 10, pp. 2003–2007, Oct. 1999.

[5] S. W. Staker, C. L. Holloway, A. U. Bhobe, and M. Piket-May, "Alternating-direction implicit (ADI) formulation of the finite-difference time-domain (FDTD) method: Algorithm and material dispersion implementation," *IEEE Trans. Electromagn. Compat.*, vol. 45, no. 2, pp. 156–166, May 2003.

[6] C. Sun and C. W. Trueman, "Unconditionally stable Crank–Nicolson scheme for solving two-dimensional Maxwell's equations," *Electron. Lett.*, vol. 39, no. 7, pp. 595–597, Apr. 2003.

[7] J. Shibayama, M. Muraki, J. Yamauchi, and H. Nakano, "Efficient implicit FDTD algorithm based on locally one-dimensional scheme," *Electron. Lett.*, vol. 41, no. 19, pp. 1046–1047, Sep. 2005.

[8] Y. Chung, T. K. Sarkar, B. H. Jung, and M. Salazar-Palma, "An unconditionally stable scheme for the finite-difference time-domain method," *IEEE Trans. Microw. Theory Techn.*, vol. 51, no. 3, pp. 697–704, Mar. 2003.

[9] E. L. Tan, "Fundamental schemes for efficient unconditionally stable implicit finite-difference time-domain methods," *IEEE Trans. Antennas Propag.*, vol. 56, no. 1, pp. 170–177, Jan. 2008.

[10] A. Ecer, N. Gopalaswamy, H. U. Akay, and Y. P. Chien, "Digital filtering techniques for parallel computation of explicit schemes," *Int. J. Comput. Fluid Dynam.*, vol. 13, no. 3, pp. 211–222, 2000.

[11] C. D. Sarris, "Extending the stability limit of the FDTD method with spatial filtering," *IEEE Microw. Wireless Compon. Lett.*, vol. 21, no. 4, pp. 176–178, Apr. 2011.

[12] C. Chang and C. D. Sarris, "A three-dimensional spatially filtered FDTD method with controllable stability beyond the Courant limit," in *IEEE MTT-S Int. Microw. Symp. Dig.*, 2012, 3 pp.

[13] Q. He, H. Gan, and D. Jiao, "Explicit time-domain finite-element method stabilized for an arbitrarily large time step," *IEEE Trans. Antennas Propag.*, vol. 60, no. 11, pp. 5240–5250, Nov. 2012.

[14] H. Gan, "Time-domain finite-element reduction-recovery methods for large-scale electromagnetics-based analysis and design of next generation integrated circuits," Ph.D. dissertation, School Elect. Comput. Eng., Purdue Univ., West Lafayette, IN, USA, 2010.

[15] Q. He and D. Jiao, "An explicit time-domain finite-element method that is unconditionally stable," in *IEEE Int. Antennas Propag. Symp.*, Jul. 2011, 4 pp.

[16] Md. Gaffar and D. Jiao, "An explicit and unconditionally stable FDTD method for 3-D electromagnetic analysis," in *IEEE MTT-S Int. Microw. Symp. Dig.*, Jun. 2013, 4 pps.

[17] I. G. Zubal, C. R. Harrell, E. O. Smith, Z. Rattner, G. Gindi, and P. B. Hoffer, "Computerized three-dimensional segmented human anatomy," *Med. Phys.*, vol. 21, no. 2, pp. 299–302, 1994.

[18] S. D. Gedney, *Introduction to the FDTD Method for Electromagnetics*. Fort Collins, CO, USA: Morgan & Claypool, 2011, pp. 50–52.

[19] D. Jiao and J. M. Jin, "A general approach for the stability analysis of time-domain finite element method," *IEEE Trans. Antennas Propag.*, vol. 50, no. 11, pp. 1624–1632, Nov. 2002.

[20] Z. Chen and P. P. Silvester, "Analytic solutions for the finite-difference time-domain and the transmission-line-matrix method," *Microw. Opt. Technol. Lett.*, vol. 7, no. 1, pp. 5–7, Jan. 1994.

[21] H. Liu and D. Jiao, "A theoretical study on the rank's dependence with electric size of the inverse finite element matrix for large-scale electrodynamic analysis," in *IEEE Int. Antennas Propag. Symp.*, Jul. 2012, pp. 1–2.

[22] W. Chai and D. Jiao, "A theoretical study on the rank of integral operators for broadband electromagnetic modeling from static to electrodynamic frequencies," *IEEE Trans. Compon., Packag., Manuf. Technol.*, vol. 3, no. 12, pp. 2113–2126, Dec. 2013.

[23] Q. He and D. Jiao, "Explicit and unconditionally stable time-domain finite-element method with a more than 'optimal' speedup," *Electromagnetics*, vol. 34, pp. 199–209, 2014.

[24] M. Gaffar and D. Jiao, "An explicit and unconditionally stable FDTD method for the analysis of general 3-D lossy problems," in *IEEE MTT-S Int. Microw. Symp. Dig.*, Jun. 2014, 4 pp.

[25] Q. He, D. Chen, J. Zhu, and D. Jiao, "Minimal-order circuit model based fast electromagnetic simulation," in *IEEE Elect. Perform. Electron. Packag. Syst. Conf.*, 2013, 6 pps.

Md. Gaffar received the B.Sc. degree in electrical engineering from the Bangladesh University of Engineering and Technology (BUET), Dhaka, Bangladesh, in 2009, and is currently working toward the Ph.D. degree in electrical and computer engineering at Purdue University, West Lafayette, IN USA.

His research interests include computational electromagnetics and semiconductor physics.

Mr. Gaffar was the recipient of academic awards in recognition of his research achievements, including the Best Poster Award (among all groups) and Best Project Award in Communication and Electromagnetic of the EEE Undergraduate Project Workshop (EUProW) 2009. At Purdue University, his research has been recognized by the 2013 IEEE International Microwave Symposium Best Student Paper Finalist Award and the 2014 IEEE International Symposium on Antennas and Propagation Honorable Mention Paper Award.

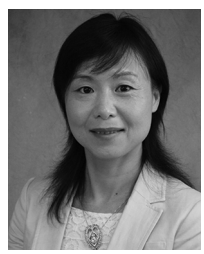

Dan Jiao (S'00–M'02–SM'06) received the Ph.D. degree in electrical engineering from the University of Illinois at Urbana-Champaign, Urbana, IL, USA, in 2001.

She then joined the Technology Computer-Aided Design (CAD) Division, Intel Corporation, until September 2005, as a Senior CAD Engineer, Staff Engineer, and Senior Staff Engineer. In September 2005, she joined Purdue University, West Lafayette, IN, USA, as an Assistant Professor with the School of Electrical and Computer Engineering, where she is currently a Professor. She has authored three book chapters and over 200 papers in refereed journals and international conferences. Her current research interests include computational electromagnetics, high-frequency digital, analog, mixed-signal, and RF integrated circuit (IC) design and analysis, high-performance very large scale integration (VLSI) CAD, modeling of microscale and nanoscale circuits, applied electromagnetics, fast and high-capacity numerical methods, fast time-domain analysis, scattering and antenna analysis, RF, microwave, and millimeter-wave circuits, wireless communication, and bio-electromagnetics.

Dr. Jiao has served as the reviewer for many IEEE journals and conferences. She is an associate editor for the IEEE TRANSACTIONS ON COMPONENTS, PACKAGING, AND MANUFACTURING TECHNOLOGY. She was the recipient of the 2013 S. A. Schelkunoff Prize Paper Award of the IEEE Antennas and Propagation Society, which recognizes the Best Paper published in the IEEE TRANSACTIONS ON ANTENNAS AND PROPAGATION during the previous year. She has been named a University Faculty Scholar by Purdue University since 2013. She was among the 85 engineers selected throughout the nation for the National Academy of Engineering's 2011 US Frontiers of Engineering Symposium. She was the recipient of the 2010 Ruth and Joel Spira Outstanding Teaching Award, the 2008 National Science Foundation (NSF) CAREER Award, the 2006 Jack and Cathie Kozik Faculty Start Up Award (which recognizes an outstanding new faculty member of the School of Electrical and Computer Engineering, Purdue University), a 2006 Office of Naval Research (ONR) Award under the Young Investigator Program, the 2004 Best Paper Award presented at the Intel Corporation's annual corporate-wide technology conference (Design and Test Technology Conference) for her work on a generic broadband model of high-speed circuits, the 2003 Intel Corporation's Logic Technology Development (LTD) Divisional Achievement Award, the Intel Corporation's Technology CAD Divisional Achievement Award, the 2002 Intel Corporation's Components Research, the Intel Hero Award (Intel-wide she was the tenth recipient), the Intel Corporation's LTD Team Quality Award, and the 2000 Raj Mittra Outstanding Research Award presented by the University of Illinois at Urbana-Champaign.